

Emergent Spectral Form Factors in Sonic Systems

Michael Winer¹ and Brian Swingle²

¹Joint Quantum Institute, Department of Physics, University of Maryland, College Park, Maryland 20742, USA

²Department of Physics, Brandeis University, Waltham, Massachusetts 02453, USA

March 29, 2025

Abstract

We study the spectral form factor (SFF) for hydrodynamic systems with a sound pole, a large class including any fluid with momentum conservation and energy conservation, or any extended system with spontaneously broken continuous symmetry. We study such systems in a finite volume cavity and find that the logarithm of the hydrodynamic enhancement is closely related to the spectral form factor of a quantum particle moving in the selfsame cavity. Depending upon the dimensionality and nature of the effective single-particle physics, we exhibit a range of behaviors including an intricate resonance phenomenon, emergent integrability in the SFF, and anomalously large fluctuations of the SFF.

1 Introduction

The statistics of the energy spectrum is one of the most important diagnostics of quantum chaos [1, 2, 3]. There is strong evidence that ensembles of chaotic systems have the same Hamiltonian spectral statistics as ensembles of Gaussian random matrices, with examples including nuclear systems [4, 5], condensed matter systems [6, 7, 8], and holographic models [9, 10]. A central quantity in spectral statistics is the Spectral Form Factor (SFF). This quantity diagnoses whether energy levels repel as they do in random matrices [6], have independent Poissonian statistics [11], or have some more exotic behavior [12, 13, 14]. The SFF can be written as

$$\text{SFF}(T, f) = \overline{|\text{Tr}[U(T)f(H)]|^2}, \quad (1)$$

where $U(T) = e^{-iHT}$ is the time evolution operator, f is a filter function (perhaps a Gaussian centered on a specific energy band), and overline denotes a disorder average over an ensemble of Hamiltonians. These Hamiltonians can differ either through microscopic disorder or, as we will see, through the overall shape of a cavity. For a discussion of how different the Hamiltonians must be to constitute “sufficient coverage”, see [15, 16, 17, 18, 19]. This disorder average is necessary because while the disorder-averaged SFF has smooth behavior as seen below, the SFF of a single Hamiltonian is highly erratic.

In [20, 21], the authors set forth a hydrodynamic theory of the spectral form factor. This effective theory predicts pure random matrix behavior at late time and computes corrections at earlier times due to slow modes. In particular, approximate symmetries enhance the ramp by an amount exponential in system size, consistent with [12, 22, 23]. This enhancement factor was calculated for simple models of a system with conserved modes and with spontaneous symmetry breaking. These calculations included tree-level effects and diagrammatic corrections not seen in traditional hydrodynamics. [20] dealt exclusively with theories first order in time, and [21] dealt with systems with no spatial extent. However, the problem of hydrodynamic systems with sound poles was left unstudied. In this work, we fill in this gap, pointing out that sound pole effects can lead to phenomena such as exponentially increasing SFFs and spectral form factors with sensitive qualitative dependence on the precise shape of the system.

In the case of 1d hydrodynamics, we find that patterns of interference impart an intricate fractal structure on the graph of the spectral form factor, as seen in figure 4. More generally, for cavities in higher dimensions,

one sees an enhancement factor that is qualitatively exponential in the single-particle SFF for a billiard of the same shape as the cavity. This means that spectral hydrodynamics for local disordered systems in integrable cavities such as tori or ellipsoids is qualitatively different than in a Bunimovich stadium or concave cavity.

The rest of the paper is organized as follows. In the remainder of the introduction, we briefly review the SFF. In Section 2, we review the hydrodynamic theory of [20] and discuss its application to systems with a sound pole. In Section 3, we treat a one-dimensional system where the SFF exhibits an intricate fractal structure. In Section 4, we move to higher dimensions and discuss the case of a sound pole when the system is confined to an integrable cavity. In Section 5, we discuss the analogous problem in a chaotic cavity. In Section 6, we discuss interaction effects, with the preceding discussion all at the quadratic level. This is followed by a brief discussion of the results; appendix A also contains a comparison to our prior work on SYK2.

Before proceeding to the derivations of these results, we first review the SFF in more detail. The SFF is closely related to the correlation function of the density of states. Formally, the (filtered) density of states is given by

$$\rho(E, f) \equiv \sum_n f(E_n) \delta(E - E_n) = \text{Tr} f(H) \delta(E - H), \quad (2)$$

where n labels the eigenstate of H with eigenvalue E_n , and its correlation function is

$$C(E, \omega, f) \equiv \mathbb{E} \left[\rho \left(E + \frac{\omega}{2}, f \right) \rho \left(E - \frac{\omega}{2}, f \right) \right]. \quad (3)$$

We have that

$$\begin{aligned} \text{SFF}(T, f) &= \mathbb{E} \left[\text{Tr} f(H) e^{-iHT} \text{Tr} f(H) e^{iHT} \right] \\ &= \int dE d\omega e^{-i\omega T} \mathbb{E} \left[\text{Tr} f(H) \delta \left(E + \frac{\omega}{2} - H \right) \text{Tr} f(H) \delta \left(E - \frac{\omega}{2} - H \right) \right] \\ &= \int d\omega e^{-i\omega T} \int dE C(E, \omega, f). \end{aligned} \quad (4)$$

The SFF is simply the Fourier transform of the correlation function with respect to ω .

The SFF can be split into two contributions:

$$\text{SFF}(T, f) = |\mathbb{E} \text{Tr} f(H) e^{-iHT}|^2 + \left(\mathbb{E} \left[|\text{Tr} f(H) e^{-iHT}|^2 \right] - |\mathbb{E} \text{Tr} f(H) e^{-iHT}|^2 \right). \quad (5)$$

The first term, the disconnected part of the SFF, comes solely from the average density of states. It is the absolute value square of the density's Fourier Transform.

It is the second term, the connected part of the SFF, that contains interesting information on the correlation between energy densities. ‘‘Random matrix universality’’ [2, 24] is the principle that an ensemble of quantum chaotic Hamiltonians will generically have the same *connected* SFF as the canonical Gaussian ensembles of random matrix theory [3, 25]. This behavior is illustrated in Fig. 1, which plots the disorder-averaged SFF of the Gaussian unitary ensemble (one of the aforementioned canonical ensembles). The graph shows the three regimes of the random matrix theory SFF:

- The ‘‘dip’’, occurring at early times, comes from the disconnected piece of the SFF (and thus its precise shape is non-universal and depends on the details of f and the thermodynamics of the system). Its downward nature reflects a loss of constructive interference — the different terms of $\text{Tr} e^{-iHT}$ acquire different phase factors as T increases.
- The ‘‘ramp’’, occurring at intermediate times, is arguably the most interesting regime. In the canonical matrix ensembles, it is a consequence of the result [3]

$$\mathbb{E} \left[\rho \left(E + \frac{\omega}{2} \right) \rho \left(E - \frac{\omega}{2} \right) \right] - \mathbb{E} \left[\rho \left(E + \frac{\omega}{2} \right) \right] \mathbb{E} \left[\rho \left(E - \frac{\omega}{2} \right) \right] \sim -\frac{1}{\mathfrak{b}\pi^2\omega^2}, \quad (6)$$

where $\mathfrak{b} = 1, 2, 4$ for the orthogonal, unitary, and symplectic ensembles respectively [3]. The fact that the right hand side is negative is known as level repulsion in quantum chaotic systems [5]. Taking the Fourier transform with respect to ω gives a term proportional to T for the connected SFF. Such a linear-in- T ramp is often taken as a defining signature of quantum chaos.

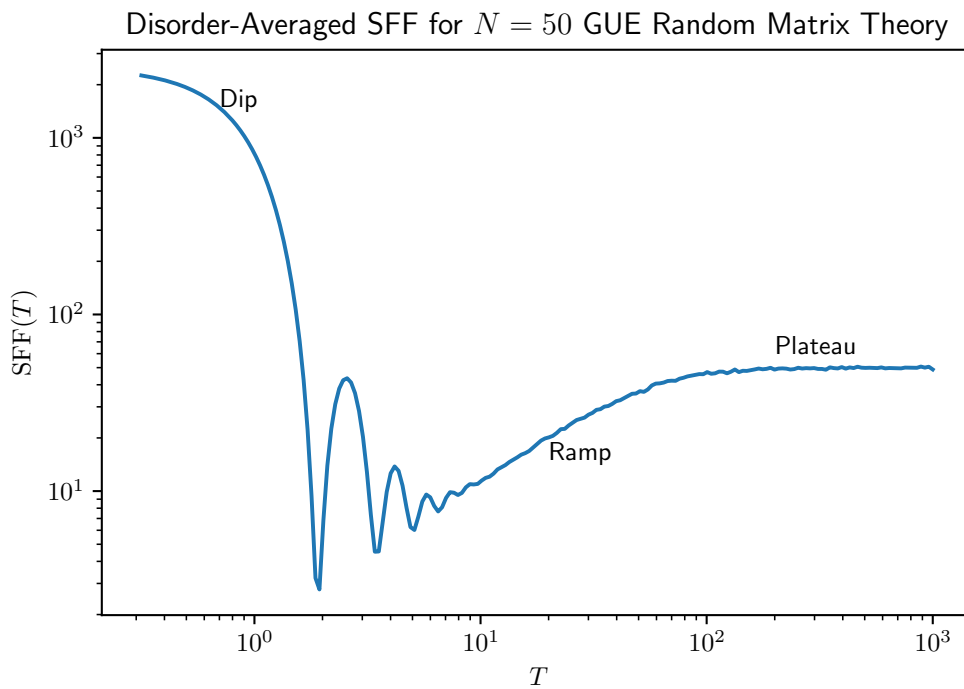


Figure 1: The disorder-averaged SFF for the Gaussian unitary ensemble (GUE). The matrices in this ensemble have dimension $N = 50$. The SFF was computed numerically by averaging over ten thousand realizations. The three regimes — dip, ramp, plateau — are labeled.



Figure 2: The Schwinger-Keldysh contour has a thermal circle of inverse temperature β and forward and backwards time evolution legs.

- The “plateau”, occurring at late times, is a fundamental consequence of the discreteness of the spectrum. At times much larger than the inverse level spacing or “Heisenberg time”, one expects that all off-diagonal terms in the double-trace of the SFF average to zero, meaning that

$$\text{SFF}(T, f) \approx \sum_{mn} e^{-i(E_m - E_n)T} f(E_m) f(E_n) \sim \sum_n f(E_n)^2. \quad (7)$$

For integrable systems, the plateau is reached very quickly with little to no ramp regime [11, 13, 14], whereas for chaotic systems it isn’t reached until a time exponential in system size. Nonetheless, it is the long-term fate of any system without a degenerate spectrum.

2 Overview of the Hydrodynamic Spectral Form Factor

2.1 Quick Review of CTP Formalism

Hydrodynamics is the program of creating effective field theories (EFTs) for systems based on the principle that long-time and long-range physics is driven primarily by conservation laws and other protected slow modes. One particularly useful formulation is the CTP formalism explained concisely in [26] and in more detail in [27, 28, 29]. Other approaches to fluctuating hydrodynamics can be found in [30, 31, 32, 33].

The CTP formalism lives on the Schwinger-Keldysh contour, pictured in figure 2. Its central object of study is the partition function

$$Z[A_1^\mu(t, x), A_2^\mu(t, x)] = \text{tr} \left(e^{-\beta H} \mathcal{P} e^{i \int dt d^d x A_1^\mu j_{1\mu}} \mathcal{P} e^{-i \int dt d^d x A_2^\mu j_{2\mu}} \right), \quad (8)$$

where \mathcal{P} is a path ordering on the Schwinger-Keldysh contour. The j operators are local conserved currents.

For $A_1 = A_2 = 0$, Z reduces to thermal partition function at inverse temperature β . Differentiating Z with respect to the A s generates insertions of the conserved current density j_μ along either leg of the Schwinger-Keldysh contour. Thus Z is the generating function of all possible contour-ordered correlation functions of current operators.

One can write Z as

$$Z[A_1^\mu, A_2^\mu] = \int \mathcal{D}\phi_1^i \mathcal{D}\phi_2^i \exp \left(i \int dt dx W[A_{1\mu}, A_{2\mu}, \phi_1^i, \phi_2^i] \right), \quad (9)$$

for some collection of local fields ϕ s. The fundamental insight of hydrodynamics is that at long times and distances, any massive ϕ s can be integrated out. All that’s left over is one ϕ per contour to enforce the conservation law $\partial^\mu j_{i\mu} = 0$. Our partition function can be written

$$Z[A_1^\mu, A_2^\mu] = \int \mathcal{D}\phi_1 \mathcal{D}\phi_2 \exp \left(i \int dt dx W[B_{1\mu}, B_{2\mu}] \right), \quad (10)$$

$$B_{i\mu}(t, x) = \partial_\mu \phi_i(t, x) + A_{i\mu}(t, x).$$

Insertions of the currents are obtained by differentiating Z with respect to the background gauge fields $A_{i\mu}$. A single such functional derivative gives a single insertion of the current, and so one presentation of current conservation is the identity $\partial_\mu \frac{\delta Z}{\delta A_{i\mu}} = 0$.

The functional W satisfies a number of constraints. The most important is locality. There are no slow modes besides ϕ , and at long enough distance and time scales integrating out fast modes should yield a local action depending on $B_{1,2}$. There are several additional constraints following from unitarity. They are best expressed in terms of

$$\begin{aligned} B_a &= B_1 - B_2, \\ B_r &= \frac{B_1 + B_2}{2}. \end{aligned} \tag{11}$$

The key constraints, which will not be proven here but are proven in, say, [27], are:

- All terms in W have at least one factor of B_a , that is $W = 0$ when $B_a = 0$.
- Terms odd (even) in B_a make a real (imaginary) contribution to the action.
- All imaginary contributions to the action are positive imaginary (or zero).
- Any correlator in which the chronologically last variable has a -type will evaluate to 0 (known as the last time theorem or LTT).
- A KMS constraint imposing fluctuation-dissipation relations.
- Unless the symmetry is spontaneously broken, all factors of B_r have at least one time derivative. This condition will be lifted in this paper, as we will be considering systems with a spontaneously broken symmetry.

For many applications including calculating SFFs, one typically sets the external sources A to zero, so the action can be written purely in terms of the derivatives of the ϕ s.

The ϕ s often have a physical interpretation depending on the precise symmetry in question. In the case of time translation, the ϕ s are the physical time corresponding to a given fluid time (and are often denoted σ). In the case of a U(1) internal symmetry, they are local fluid phases. One simple quadratic action for an energy-conserving system consistent with the above conditions is

$$L = \sigma_a (\kappa\beta^{-1}\partial_t^2\sigma_r - D\kappa\beta^{-1}\nabla^2\partial_t\sigma_r) + i\beta^{-2}\kappa(\nabla\sigma_a)^2. \tag{12}$$

2.2 The DPT Formalism and the SFF

The SFF (or at least the ramp portion) for a system with one diffusive mode can be calculated by evaluating the path integral

$$\text{SFF} = \int \mathcal{D}\sigma_1 \mathcal{D}\sigma_2 f(E_1) f(E_2) e^{iS_{\text{hydro}}(\sigma_1, \sigma_2)}, \tag{13}$$

where $\sigma_{1,2}$ represent reparameterization modes on the two legs of the contour. We define

$$\begin{aligned} \sigma_a &= \sigma_1 - \sigma_2 \\ \rho &= \frac{\partial S}{\partial(\partial_t\sigma_a)}. \end{aligned} \tag{14}$$

Here ρ is the average energy density on the two contours. We can write

$$L = -\sigma_a (\partial_t\rho - D\nabla^2\rho) + i\beta^{-2}\kappa(\nabla\sigma_a)^2. \tag{15}$$

Since the action is entirely Gaussian, we can evaluate the path integral exactly. We first break into Fourier modes in the spatial directions. The remaining integral is

$$\prod_k \int \mathcal{D}\epsilon_k \mathcal{D}\sigma_{ak} f(E_1) f(E_2) \exp\left(-i \int dt \sigma_{ak} \partial_t \rho_k + Dk^2 \sigma_{ak} \rho_k - \beta^{-2} \kappa k^2 \sigma_{ak}^2\right) \tag{16}$$

For $k \neq 0$, breaking the path integral into time modes gives an infinite product which evaluates [20] to $\frac{1}{1-e^{-Dk^2T}}$. For $k = 0$, we just integrate over the full manifold of possible σ_a s and ρ_s to get $\frac{T}{2\pi} \int f^2(E)dE$. So the full connected SFF for systems with a single diffusive mode is

$$\text{SFF} = \prod_k \frac{1}{1-e^{-Dk^2T}} \frac{T}{2\pi} \int f^2(E)dE. \quad (17)$$

In the large-volume thermodynamic limit, this product can be evaluated by taking the log and then Taylor expanding $\log(1-e^{-Dk^2T})$. The result is

$$\log \text{SFF} = V \left(\frac{1}{4\pi DT} \right)^{d/2} \zeta(1+d/2), \quad (18)$$

where $\zeta(s) = \sum_{n=1}^{\infty} \frac{1}{n^s}$ is the famous Riemann zeta function.

For more complicated systems with multiple slow modes and more general dispersion relations than $\omega = iDk^2$ we have

$$\text{SFF} = \prod_{\text{Slow Modes } \phi_j} \prod_k \frac{1}{1-e^{i\omega_j(k)T}} \frac{T}{2\pi} \int f^2(E)dE. \quad (19)$$

In terms of the random matrix form factor,

$$\text{SFF}_{\text{GUE}} = \frac{T}{2\pi} \int f^2(E)dE, \quad (20)$$

the enhancement factor is simply

$$Z_{\text{enhancement}} = \frac{\text{SFF}}{\text{SFF}_{\text{GUE}}} = \prod_{\text{Slow Modes } \phi_j} \prod_k \frac{1}{1-e^{i\omega_j(k)T}}. \quad (21)$$

We will compute this quantity for a variety of systems with a sound below.

2.3 DPT Formulation For Sonic Systems

We are finally ready to tackle the problem of sound poles SFF hydrodynamics. We start with a Lagrangian

$$L = \frac{1}{2} \phi_a \left(\partial_t^2 + \frac{2\Gamma}{c^2} \partial_t^3 - c^2 \partial_\mu^2 \right) \phi_r + \frac{2i\Gamma}{\beta c^2} \phi_a \partial_t^2 \phi_a + \text{higher derivative terms}. \quad (22)$$

This sort of Lagrangian might arise in a superfluid, where ϕ plays the role of an order parameter. Alternatively this can be taken as a minimal schematic for a system with a more conventional sound pole, such as familiar fluid systems with energy and momentum conservation.

In general this Lagrangian is cubic in frequency, and the equations of motion gives us three solutions for ω . For small k^2 , these solutions are $\omega = \pm ck + i\Gamma k^2, i\frac{2\Gamma}{c^2}$. This last mode is fast, and can be ignored in the infrared. So the SFF enhancement is

$$\log Z_{\text{enhancement}} = - \sum_{k^2 \text{ eigenvalue of Laplacian, } \mathfrak{s}=\pm} \log(1 - \exp\{i\mathfrak{s}ck - \Gamma k^2\}T). \quad (23)$$

By Taylor expanding the log on the right, we also have

$$\log Z_{\text{enhancement}} = \sum_{j=1}^{\infty} \sum_{k^2, \mathfrak{s}} \frac{\exp(j(i\mathfrak{s}ck - \Gamma k^2)T)}{j}. \quad (24)$$

The presence of the complex exponentials in equation (24) leads to qualitatively new behavior. While purely diffusive systems see $Z_{\text{enhancement}}$ decay monotonically as T increases, in sonic systems we see an intricate interplay between the positive and negative terms in (24).

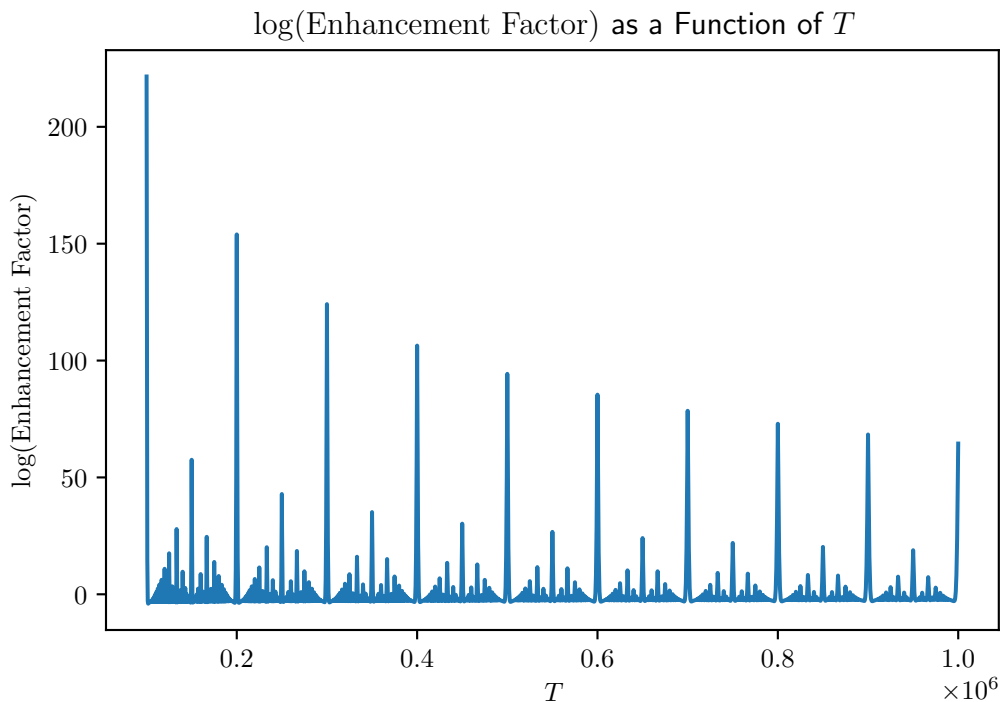


Figure 3: The log of the SFF enhancement factor for a system of length $L = 10^6$ with $c = 1$, $\Gamma = 1$. The graph cuts off at a lower bound of $T = 1,000,000$, otherwise the $T = 0$ divergence would overwhelm the rest of the image.

3 Babylon: The 1D Sound Pole

In this section we will concern ourselves with the SFF enhancement for a 1D system with periodic boundary conditions. In this case, the k s are just $2\pi n/L$. We can evaluate equation (23) numerically. For a particular parameter choice, the results are shown in figure 3.

Before we can understand this fascinating picture, we need to discuss the function

$$f(x) = \begin{cases} \frac{1}{n} & \text{if } x = \frac{m}{n} \quad (x \text{ is rational}), \text{ with } m \in \mathbb{Z} \text{ and } n \in \mathbb{N} \text{ coprime} \\ 0 & \text{if } x \text{ is irrational.} \end{cases} \quad (25)$$

This function is known by many names fanciful names including the popcorn function, the raindrop function, the countable cloud function, and, best of all, the Stars over Babylon.

What does this fairytale function have to do with function in equation (23)? The answer is that there is a huge enhancement whenever the system is in resonance, that is whenever $cT/L = m/n$. Setting $k = 2\pi q/L$ and imposing the resonance condition, the sum becomes

$$\log Z_{\text{enhancement}} = -2 \sum_{q>0, s=\pm} \log \left(1 - \exp \left\{ \left(2\pi i s \frac{mq}{n} - \Gamma k^2 \right) T \right\} \right), \quad (26)$$

so every n th term in the sum over n_k contributes a term $-\log(1 - \exp(-\Gamma k^2 T))$, which is very close to $-\log 0$ when k is small. Since only a $1/n$ fraction of the modes contribute, and contributions like this swamp out any others, we get a structure like equation (25). A more careful accounting in the next subsection will reveal that the Babylon formula is actually modified to $n^{-3/2}$ from $1/n$.

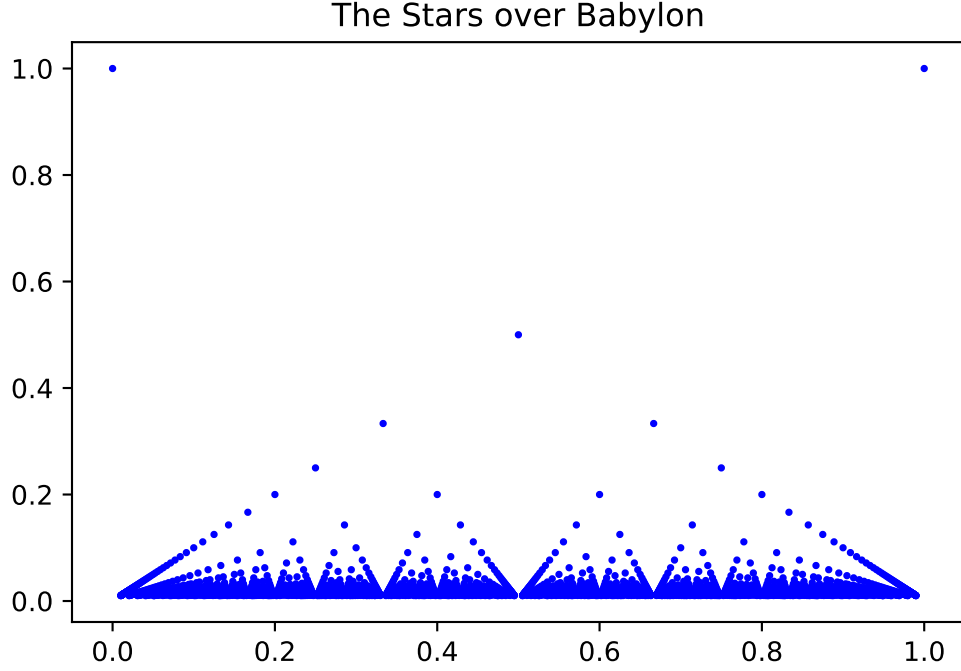


Figure 4: The Stars over Babylon. The Stars over Babylon function in this range corresponds to one period in figure 3.

3.1 Details on the 1D SFF

Not content to observe the Stars over Babylon pattern, let's work out some quantitative details. For instance, how tall should one expect the peaks at full resonance to be? These are the times T satisfying $cT/L = m$ for some integer m . So we have

$$\log Z_{\text{enhancement}}(T = mL/c) = -2 \sum_{q \in \mathbb{N}/\{0\}} \log \left(1 - \exp \left(-\Gamma \left(\frac{2\pi q}{L} \right)^2 T \right) \right) \quad (27)$$

If we replace Γ with D , we see that at these special resonant times, this is also the enhancement factor for normal diffusion. So for times $T \ll L^2/\Gamma$ we can thus use the same methods leading to (18) to get

$$\log Z_{\text{enhancement}} \left(T = \frac{mL}{c} \right) = 2L \left(\frac{1}{4\pi\Gamma T} \right)^{1/2} \zeta(3/2). \quad (28)$$

For a picture of this envelope versus the actual function, see figure 5. We can also evaluate an envelope for the shorter peaks for $n > 1$. In these cases it is best to break the sum into sets of n consecutive terms. We can write this exactly as

$$\log Z_{\text{enhancement}} \left(T = \frac{mL}{nc} \right) = - \sum_{q \in \mathbb{N}/\{0\}, s = \pm} \sum_{q_2=0}^{n-1} \log \left(1 - \exp \left(-\Gamma \left(\frac{2\pi(nq - q_2)}{L} \right)^2 T + \mathfrak{s} 2\pi i q_2/n \right) \right). \quad (29)$$

In the thermodynamic limit $cL \gg \Gamma$ we can treat the Gaussian as constant within each inner sum. We can then use the identity

$$\sum_{q=0}^{n-1} \log(1 - a \exp(2\pi i q/n)) = \log(1 - a^n) \quad (30)$$

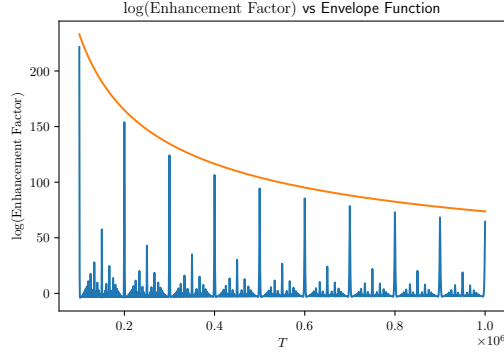


Figure 5: Equation (28) does a good job estimating the envelope for $L = 1,000,000$, $c = 1$, $\Gamma = 1$. The source of the discrepancy comes from approximating the sum in equation (27) as an integral. This approximation is valid in the limit $cL \gg \Gamma$ where many terms contribute to the sum.

to perform the inner sum. We have

$$\log Z_{\text{enhancement}} \left(T = \frac{mL}{nc} \right) = - \sum_{q \in \mathbb{N} \setminus \{0\}} \sum_{q_2=0}^{n-1} \log \left(1 - \exp \left(-n\Gamma \left(\frac{2\pi nq}{L} \right)^2 T \right) \right). \quad (31)$$

This is the same sum again but with Γ replaced with $n^3 \Gamma$. This means that we have

$$\log Z_{\text{enhancement}} \left(T = \frac{mL}{nc} \right) = L \frac{1}{n^{3/2}} \left(\frac{1}{4\pi\Gamma T} \right)^{1/2} \zeta(3/2). \quad (32)$$

This $n^{-3/2}$ is interesting and surprising. Again, in the original Babylon function, there is just an $1/n$. We justified this by saying that $1/n$ of the terms contribute exploding positive contributions to the sum. However, the other $n - 1$ terms can be shown to on average contribute slightly negative suppressing terms. This provides the intuition for the $n^{-3/2}$ in equation (32).

A final word about when these approximations become valid. Based on numerically evaluating equation (23), it seems that the spikes at integers don't become clearly visible until this system size is a thousand relaxation lengths, and the full fractal structure isn't visible until ten thousand. Figures 3 and 5 use a system size of a million. Needless to say, this is quite beyond the realm of any foreseeable exact diagonalization calculation or experimental technology.

3.2 A Fourier Perspective

The analysis in the above subsection tells us the height of the peaks, but doesn't tell us anything about their breadth or shape. We can extract this information by taking the Taylor expansion of $\log(1 - x) = \sum_{j=1}^{\infty} -\frac{1}{j} x^j$

$$\log Z_{\text{enhancement}} = 2 \sum_{q>0, s=\pm} \sum_{j=1}^{\infty} \frac{1}{j} \exp \left(2\pi i q s \frac{cT}{L} j \right) \exp \left(-j \frac{4\pi^2 \Gamma q^2}{L^2} T \right), \quad (33)$$

For each j this is the Fourier transform of a chain of tight peaks (missing a $q = 0$ term). The peaks have Gaussian shape, and recur after time $\frac{L}{cj}$. The total area under the Gaussian is given by the amplitude of the missing $q = 0$ term times the period. This is just an amplitude of $\frac{1}{j}$ times a period of $\frac{L}{cj}$ gives an area of $\frac{L}{cj^2}$.

Combined with the results of the previous subsection, we know that the width of the Gaussian is something like $\# \frac{1}{c} \sqrt{\frac{\Gamma T}{n}}$. This means that at sufficiently large n , the width of the peaks does become greater than the area between the peaks, and the lovely Stars over Babylon structure does not have infinite resolution.

3.3 Star Destroyer

It is also worth wondering how higher derivative-terms and interactions would affect the qualitative result of the Babylon-shaped enhancement factor. In the thermodynamic limit, the higher derivative terms don't substantially affect the pattern. The higher derivative terms only affect larger values of k , which are already suppressed since they have factors of $e^{-\Gamma k^2 T}$.

Interactions, however, can have a more noticeable impact. While in the CTP formalism the velocity would merely be renormalized by a smooth amount, in DPT the velocity is renormalized by an amount depending sensitively on frequency. We hypothesize that this irregularity would substantially derange the intricate pattern, likely in favor of a more erratic pattern of spikes.

4 Sound In An Integrable Cavity

We will now examine the case where the operator Laplacian in our cavity has Poissonian spectral statistics. This might occur, for instance, if the system is a torus or an ellipsoid. It is generally thought to describe the case where the cavity, when viewed as a stadium/billiard, gives rise to integrable dynamics for a particle moving inside the stadium.

For a general Poissonian system, the enhancement coefficient can be written as

$$Z_{\text{enhancement}} = \prod_{k>0, k^2 \text{ eigenvalue of Laplacian}} \frac{1}{(1 - \exp\{(ick - \Gamma k^2)T\})(1 - \exp\{(-ick - \Gamma k^2)T\})}. \quad (34)$$

Using the Poissonian statistics, we can calculate the expected value of this enhancement factor. In any Poissonian system, the density of Laplacian “energy” eigenvalues in the interval $[E_1, E_1 + \delta E_1]$ is independent of that in region $[E_2, E_2 + \delta E_2]$ for $E_1 \neq E_2$. This independence implies a similar independence for $k \sim \sqrt{E}$. So we can evaluate the expected value of equation (34) by partitioning the spectrum of k into non-overlapping regions $[k_i, k_i + \delta k]$, finding the expected value of the product over eigenvalues in that region, and then multiplying the results together.

In any given region, the product is $[(1 - \exp\{(ick - \Gamma k^2)T\})(1 - \exp\{(-ick - \Gamma k^2)T\})]^{-1}$ with probability $\bar{\rho} dk$ (eigenvalue present) and 1 with probability $1 - \bar{\rho} dk$ (eigenvalue absent). The expected value is thus

$$1 + \left(\frac{1}{(1 - \exp\{(ick - \Gamma k^2)T\})(1 - \exp\{(-ick - \Gamma k^2)T\})} - 1 \right) \bar{\rho} dk. \quad (35)$$

This means that in expectation we can write

$$\overline{Z_{\text{enhancement}}} = \exp \left(\int_0^\infty dk \left(\frac{1}{(1 - \exp\{(ick - \Gamma k^2)T\})(1 - \exp\{(-ick - \Gamma k^2)T\})} - 1 \right) \bar{\rho}(k) \right). \quad (36)$$

This formula isn't the result of a cumulant expansion, it is exact for a purely Poissonian density for k . Figure 6 shows numerics backing up this prediction. To create figure 6, we used the most Poissonian process possible: independent random numbers. It does not correspond to particular cavity shape.

It is worth noting that equation (34) is a product over many terms. As such, depending on context, the mean value might not be a good representation of typical values, for the same reason that log-normal distributions are not well-clustered around their mean. The expected value of the log of the coefficient can be calculated straightforwardly by taking the log of equation (34).

However, we emphasize that real billiard systems, even integrable ones, do not have truly Poissonian spectral statistics. The clearest exhibition of this is in the case of periodic orbits. To explain how this effects the result, consider a torus of dimensions $2\pi \times 4\pi$. The spectrum of the Laplacian is given by choosing a wavevector of the form (n_x, n_y) where n_x is integer valued and n_y can also take half-integer values. For example, one possible Laplacian eigenstate has wavevector $(1, \frac{1}{2})$, which gives $k^2 = \frac{5}{4}$, $k = \frac{\sqrt{5}}{2}$. There is another eigenstate with wavevector $(2, 1)$, which corresponds to $k = \sqrt{5}$. In general, there will be states with $k = n \frac{\sqrt{5}}{2}$ for all positive integers n . When we multiply the enhancement factors for all of these states, we get the same intricate pattern seen in figure 3.

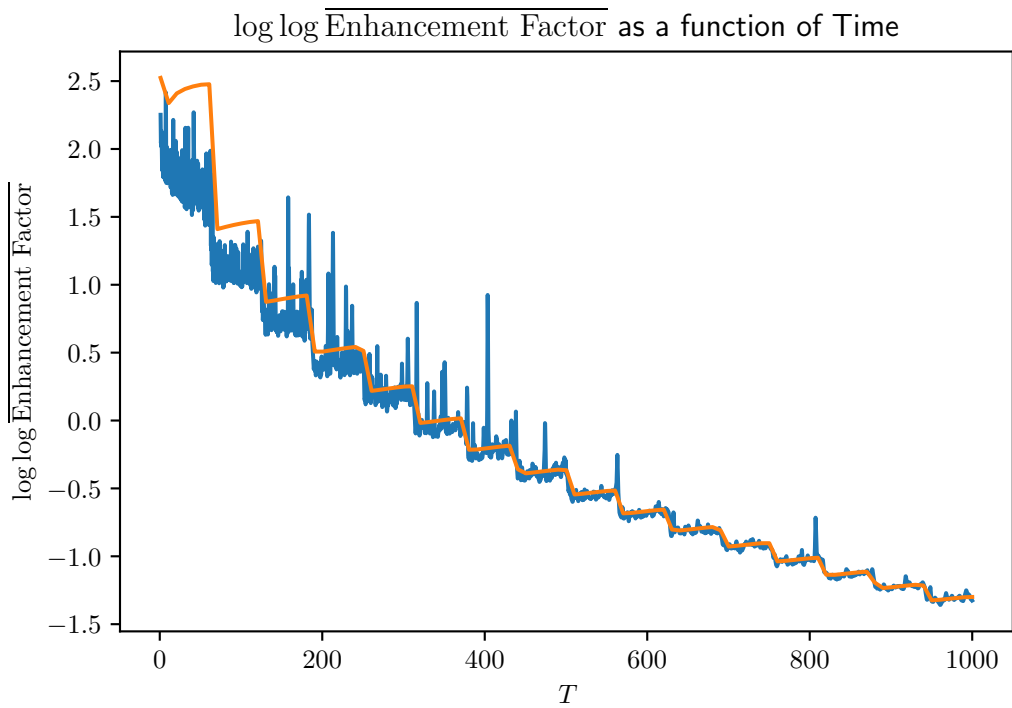


Figure 6: A graph illustrating the agreement of numerical (blue) vs theoretical (orange) predictions for equation 36. We chose $c = 1, \Gamma = 0.1, \bar{\rho}(k) = 1$. Because equation (36) has a divergence at low k we had a cutoff of $k = 0.1$. This cutoff is responsible for the interesting steplike behavior seen in both functions. The blue line is an average of 1971459 samples.

We think that this same effect can exist more generally in any cavity in which a classical particle can take a closed periodic path. To show this, we imagine that we start a quantum wavepacket moving under a fictitious Hamiltonian $H_{\text{fict}} = -\frac{1}{2m_{\text{fict}}}\nabla^2$ at velocity v around a periodic path of length L . The wavepacket does not have a definite energy, but instead a spread of energies well-centered on $E_{\text{fict}} = \frac{k^2}{2m_{\text{fict}}} = \frac{m_{\text{fict}}v^2}{2}$. If we choose a k very large compared to the inverse system size (well into the semiclassical limit) then all of the energy eigenvalues contributing to this wavepacket are close to E_{fict} .

Because the classical motion is periodic, the wavefunction is going to be approximately periodic in time with period L/v . This means that the wavepacket has overlap with H_{fict} eigenstates with energies that differ by integer multiples of $\frac{2\pi v}{L}$. So there will be values of $k = \sqrt{2m_{\text{fict}}E_{\text{fict}}}$ spaced out, separated by integer multiples of $\frac{2\pi}{L}$. These evenly spaced out modes violate our assumption of Poissonness, and will lead to contributions like in figure 3. It is likely, however that these effects will drown out after a comparatively short time once the wavefunction has time to spread out. For chaotic systems this time is known as the Ehrenfest time, and is on the order of $\frac{\log \frac{\text{Phase Space Volume}}{h^d}}{\lambda}$, where λ is the Lyapunov exponent. For integrable systems the time is given by the same star destroying effects as in section 3.3. For a generic integrable system, ω will depend on d commuting quantum numbers. The dependence will be well approximated as linear, but any higher-derivative terms in the hydro theory or dispersion in the integrable system will break that perfect interference.

5 Sound in a Chaotic Cavity

The expression for the enhancement from sound poles in a generic cavity is

$$\log Z_{\text{enhancement}} = \sum_{j=1}^{\infty} \sum_{k^2 \text{ eigenvalue of Laplacian, } \mathfrak{s}=\pm} \frac{1}{j} \exp((i\mathfrak{s}ck - \Gamma k^2)jT) \quad (37)$$

Let's imagine the shape of the cavity is a Bunimovich stadium. Then the k^2 s become the eigenvalues of a level-repelling chaotic Hamiltonian of the Gaussian Orthogonal Ensemble (GOE) universality class. So the ks are the stretched eigenvalues, but still exhibit GOE-type level repulsion.

We can view the right hand side of equation (37) as a sum over partition functions with imaginary temperature x associated with the k spectrum,

$$Z(x, f) = \int dk \rho(k) e^{ikx} f(k) \quad (38)$$

where ρ is the exact density of states and f is a filter function. In particular, we have

$$\log Z_{\text{enhancement}} = \sum_{j=1, \mathfrak{s}=\pm}^{\infty} \frac{1}{j} Z[j\mathfrak{s}cT, f_j = \exp(-j\Gamma T k^2)]. \quad (39)$$

If we fix particular stadium, then we expect that the enhancement factor will be an erratic function of time.

To get a smooth result which is calculable, we average over a number of configurations for our stadium, being careful to remain in the GOE universality class, instead of calculating the logarithm of $Z_{\text{enhancement}}$ for a given realization of the stadium. Denoting by W the quantity in equation (39), we have $\log \langle Z_{\text{enhancement}} \rangle = \log \langle e^W \rangle$, which is by definition the sum of the cumulants of W .

Doing a cumulant expansion, we get

$$\log Z_{\text{enhancement}} = \sum_{\ell} \frac{1}{\ell!} c_{\ell} = \mathbb{E} \left[\sum_{j, \mathfrak{s}} \frac{1}{j} Z(j\mathfrak{s}cT, f_j) \right] + \frac{1}{2} \text{var} \left[\sum_{j, \mathfrak{s}} \frac{1}{j} Z(j\mathfrak{s}cT, f_j) \right] + \dots \quad (40)$$

For times smaller than the Heisenberg time of the single-particle system, we can approximate the cumulant expansion with just the first two terms. We will consider these two terms in turn.

The first cumulant is obtained from the average density of states. Our system has some density of states $\rho(k)$ which fluctuates depending on the precise shape of the cavity. Averaging over such details (a step

beyond the microscopic disorder average we already performed to get a hydrodynamic theory) we get that $\rho(k)$ fluctuates about some quantity $\bar{\rho}(k)$. $\bar{\rho}$ can be calculated in a semiclassical approximation. If the cavity has d -dimensional volume V , we can expect a density of states

$$\bar{\rho}(k) = \frac{V}{(2\pi)^d} S_{d-1} k^{d-1}, \quad (41)$$

where $S_{d-1} = \frac{2\pi^{\frac{d-1}{2}}}{\Gamma(\frac{d-1}{2})}$ is the surface area of a $d-1$ sphere.

So the expected value of the imaginary-time partition function is

$$\mathbb{E} \left[\frac{1}{j} Z(j\mathfrak{s}cT, f_j = \exp(-j\Gamma Tk^2)) \right] = \frac{VS_{d-1}}{(2\pi)^d j} \int_0^\infty dk k^{d-1} \exp(ij\mathfrak{s}cTk) \exp(-j\Gamma Tk^2). \quad (42)$$

After including the sum over \mathfrak{s} and relabeling $k \rightarrow -k$ in the $\mathfrak{s} = -$ term, we have

$$\sum_{\mathfrak{s}} \mathbb{E} \left[\frac{1}{j} Z(j\mathfrak{s}cT, f_j) \right] = \frac{VS_{d-1}}{(2\pi)^d j} \int_{-\infty}^\infty dk |k|^{d-1} \exp(ij\mathfrak{s}cTk) \exp(-j\Gamma Tk^2) \quad (43)$$

Right away, we notice that the behavior is qualitatively different for even versus odd d . For odd d , we have the Fourier transform of an analytic function, while for even d , there is a non-analyticity at $k = 0$.

If we evaluate the expression, we get

$$\sum_{\mathfrak{s}} \mathbb{E} \left[\frac{1}{j} Z(j\mathfrak{s}cT, f_j) \right] = \begin{cases} \frac{VS_{d-1}}{(2\pi)^d j} \sqrt{\frac{2\pi}{j\Gamma T}} (jT)^{1-d} \partial_c^{d-1} \exp\left(-j\frac{c^2}{4\Gamma} T\right) & \text{if } d \text{ odd,} \\ \frac{2VS_{d-1}}{(2\pi)^d j} \frac{(d-1)!}{(ijcT)^d} + O(T^{-d-1}) & \text{if } d \text{ even.} \end{cases} \quad (44)$$

As we see, in odd dimensions this is an exponential decay, while in even dimensions it is a power-law decay. This is related to the fact that sound waves have sharp edges in odd dimensions and soft edges in even dimensions. The terms in (44) can be plugged into (40) and the sum over j computed to get

$$\log \overline{Z_{\text{enhancement}}} \supset \begin{cases} \frac{VS_{d-1}}{(2\pi)^d} \sqrt{\frac{2\pi}{\Gamma T}} (T)^{1-d} \partial_c^{d-1} \exp\left(-\frac{c^2}{4\Gamma} T\right) & \text{if } d \text{ odd,} \\ \zeta(d+1) \frac{2VS_{d-1}}{(2\pi)^d} \frac{(d-1)!}{(icT)^d} + O(T^{-d-1}) & \text{if } d \text{ even.} \end{cases} \quad (45)$$

If we stopped here, at the first term in the cumulant expansion, we would be making the approximation $\log \overline{Z_{\text{enhancement}}} = \overline{\log Z_{\text{enhancement}}}$. By analogy with the glass literature, we refer to $\log \overline{Z_{\text{enhancement}}}$ as the annealed case and $\overline{\log Z_{\text{enhancement}}}$ as the quenched case. The above approximation is thus analogous to the approximation that quenched equals annealed. Typically, the quenched value of a partition function is the value for a typical realization of disorder, whereas the unquenched or annealed value is dominated by more extreme terms. If one were to take a small number of cavity shapes and evaluate the SFF enhancement coefficients, most of the coefficients would look like equation (45). This is because we have $\log Z_{\text{enhancement}} \sim \rho$ sample by sample, so the quenched average contains only a linear-in- ρ term whereas the annealed average has contributions from higher cumulants. Equation (45) also gives the quenched answer for an integrable system.

Now onto the second cumulant, which for the j th partition function is

$$\text{var} \left[\sum_{j,\mathfrak{s}} \frac{1}{j} Z(j\mathfrak{s}cT, f_j) \right] = \sum_{j,j',\mathfrak{s},\mathfrak{s}'} \frac{1}{jj'} \int dk dk' \mathbb{E}(\rho(k)\rho(k'))_{\text{conn}} e^{ij\mathfrak{s}cT + ij'k's'cT} f_j(k) f_{j'}(k'), \quad (46)$$

where $\mathbb{E}(\rho(k)\rho(k'))_{\text{conn}}$ is the connected pair correlation function. Further progress can be made under the assumption that the connected correlator has only weak dependence on $k+k'$. In this case, only terms with $j = j'$ and $\mathfrak{s} = -\mathfrak{s}'$ contribute, giving

$$\text{var} \left[\sum_{j,\mathfrak{s}} \frac{1}{j} Z(j\mathfrak{s}cT, f_j) \right] \approx \frac{1}{j^2} \sum_{j,\mathfrak{s}} \int dk dk' \mathbb{E}(\rho(k)\rho(k'))_{\text{conn}} e^{ij\mathfrak{s}(k-k')cT} f_j(k) f_j(k'). \quad (47)$$

Now, this expression is essentially a sum over single-particle spectral form factors evaluated at the times jcT and with filter function f_j . For each of these we may use the standard GOE result to obtain

$$\text{var} \left[\sum_{j,s} \frac{1}{j} Z(j\mathfrak{s}cT, f_j) \right] \approx \sum_j \frac{2}{j^2} \int_0^\infty d\bar{k} \left(\frac{jcT}{\pi} \right) \exp(-2j\Gamma T \bar{k}^2). \quad (48)$$

The integral is straightforward, and the total variance is thus

$$\text{var} \left[\sum_{j,s} \frac{1}{j} Z(j\mathfrak{s}cT, f_j) \right] \approx \sum_j \frac{cT}{j\pi} \sqrt{\frac{\pi}{2j\Gamma T}} = \zeta(3/2) \sqrt{\frac{c^2 T}{2\pi\Gamma}}. \quad (49)$$

This answer is eerily reminiscent of equation (28). But most interestingly, it is a highly universal contribution to the ramp of a hydrodynamic system with a sound pole. It doesn't depend on any details of the shape of the system, or even its overall size. Just that the sound waves propagating around experience chaotic dynamics.

Equation (49) increases indefinitely, and it is worth knowing when exactly it starts to fail. The answer is that at times on the order of the single-particle Heisenberg time (inverse level spacing of the single-particle system) the second cumulant reaches a plateau, and cumulants after the second stop being negligible. After a few Heisenberg times, there is no longer any residue of the single-particle level repulsion and the enhancement for chaotic billiards should resemble that for integrable billiards. In summary, here is a list of important time scales for the connected sound pole SFF in a chaotic cavity:

- Hydrodynamic scattering time of order Γ/c^2 . In odd dimensions, this is the time scale for the connected part of the SFF enhancement factor to decay. Before this time, equation (45) represents the dominant contribution to the SFF enhancement in all numbers of dimensions.
- Single particle Thouless time, on the order of L/c . This is the time scale at which equation (49) becomes a good approximation.
- The single particle Heisenberg scale on the order of $\left(\frac{1}{c}\Gamma^{-\frac{d-1}{2}}\right)^{\frac{2}{d+1}}$. Equation (49) is dominated by modes with k on the order of $k \sim (\Gamma T)^{-1/2}$. The single particle Heisenberg scale is the time at which T exceeds the density of states in this region. Above this time scale a chaotic billiard should behave like an integrable billiard.
- The many-body Heisenberg time at order e^S . This is the time scale at which the SFF of the full many-body system plateaus.

6 Interactions

In this section, we sketch the inclusion of hydrodynamic interactions using a diagrammatic perturbation theory along the lines discussed in [20]. We consider the basic diagrammatic setup and, as an example, evaluate a single diagram. We do not give a comprehensive analysis of interaction effects and discuss some key open issues at the end of the section.

Let's enhance our action to include interactions among the various modes. We now have a Lagrangian that includes a huge number of possible cubic and higher-order interactions. This leads to perturbative corrections to $\log Z_{\text{enhancement}}$. For concreteness, we will choose the Lagrangian

$$L = \frac{1}{2} \phi_a \left(\partial_t^2 + \frac{2\Gamma}{c^2} \partial_t^3 - c^2 \partial_\mu^2 \right) \phi_r + \frac{2i\Gamma}{\beta c^2} \phi_a \partial_t^2 \phi_a + \lambda (\partial_\mu \phi_r)^2 \partial_t \phi_r \partial_t \phi_a, \quad (50)$$

though there are other quadratic terms with comparable effects.

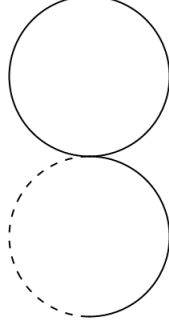


Figure 7: The dashed line represents ϕ_a , the solid line represents ϕ_r .

We evaluate these terms diagrammatically, according to the rules in [20]. The propagators in the CTP formalism are

$$G_{ra}^{CTP}(t, k) = \text{Re} \frac{e^{-\Gamma k^2 t}}{ic|k| - \Gamma k^2} \exp(ic|k|t) \theta(t), \quad (51)$$

$$G_{rr}^{CTP}(t, k) = \text{Re} \frac{e^{-\Gamma k^2 |t|}}{ic|k| - \Gamma k^2} \exp(ic|k||t|).$$

In the DPT formalism, propagators are wrapped around the time circle according to

$$G^{DPT}(t, k) = \sum_{n=-\infty}^{\infty} G^{CTP}(t + nT, k). \quad (52)$$

Note that the IR divergence for a sound-pole system is much less pronounced than in the case of diffusive hydrodynamics.

With our propagators in hand, it is time to evaluate Feynman diagrams. Since the SFF is a partition function on an unorthodox manifold, the correction to the log of the SFF is given by a sum of bubble diagrams. The leading diagram is given in figure 7. This can be factored to

$$\Delta L = -\lambda \left(\int d^d k_1 k_1^2 G_{rr}^{DPT}(t=0, k_1) \right) \left(\int d^d k_2 \partial_t^2 G_{ra}^{DPT}(t=0, k_2) \right) \quad (53)$$

The first of the integrals is UV divergent. We will impose a hard cutoff at $k = \Lambda$. In keeping with realistic hydrodynamics, we will chose $\Lambda \ll \frac{c}{\Gamma}$. With this cutoff, the first integral works out to $\frac{S_{d-1}}{d+2} \frac{\Gamma}{c^2} \Lambda^{d+2}$. The second integral can be evaluated as

$$\begin{aligned} \int d^d k_2 \partial_t^2 G_{ra}^{DPT}(t=0, k) &= \sum_{j=1}^{\infty} \int d^d k \partial_t^2 G_{ra}^{CTP}(jT, k) = \text{Re} \sum_{j=1}^{\infty} \int d^d k (ic|k| - \Gamma k^2) e^{-j\Gamma k^2 T} \exp(ijc|k|T) = \\ &S_{d-1} \text{Re} \sum_{j=1}^{\infty} \int_0^{\infty} dk (ick - \Gamma k^2) |k|^{d-1} e^{-j\Gamma k^2 T} \exp(ijckT) = \\ &\frac{S_{d-1}}{2} \sum_{j=1}^{\infty} \int_{-\infty}^{\infty} dk (ick - \Gamma k^2) |k|^{d-1} e^{-j\Gamma k^2 T} \exp(ijckT) \end{aligned} \quad (54)$$

Much like equation (44), the integral in equation (54) has long-time behavior if d is even, and a quick decay if d is odd. The integral works out to

$$\int_{-\infty}^{\infty} dk (ick - \Gamma k^2) |k|^{d-1} e^{-j\Gamma k^2 T} \exp(ijckT) = \begin{cases} \sqrt{\frac{2\pi}{j\Gamma T}} \left(c \frac{1}{(jT)^d} \partial_c^d - \Gamma \frac{1}{(jT)^{d+1}} \partial_c^{d+1} \right) \exp\left(-j \frac{c^2}{4\Gamma} T\right) & \text{if } d \text{ odd} \\ c \frac{(d)!}{(ijcT)^{d+1}} + O(T^{-d-2}) & \text{if } d \text{ even} \end{cases} \quad (55)$$

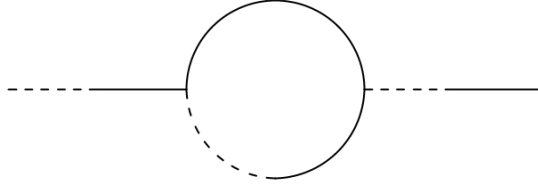


Figure 8: The loop integral in this diagram depends on the second moment of the spectral density.

For odd d , the sum in equation (54) is dominated by the $j = 1$ term, while for even d we extract a value of $c\zeta(d+1)\frac{(d)!}{(icT)^{d+1}} + O(T^{-d-2})$.

Multiplying everything together, we get

$$\Delta S/(VT) \approx \begin{cases} -\lambda \frac{S_{d-1}^2}{2(d+2)} \frac{\Gamma}{c^2} \Lambda^{d+2} \sqrt{\frac{2\pi}{\Gamma T}} \left(c \frac{1}{(T)^d} \partial_c^d - \Gamma \frac{1}{(T)^{d+1}} \partial_c^{d+1} \right) \exp\left(-\frac{c^2}{4\Gamma T}\right) & \text{if } d \text{ odd,} \\ -\lambda \frac{S_{d-1}^2}{2(d+2)} \frac{\Gamma}{c} \Lambda^{d+2} \zeta(d+1) \frac{(d)!}{(icT)^{d+1}} & \text{if } d \text{ even.} \end{cases} \quad (56)$$

This can be interpreted as a renormalization of c in equation (44). More complicated diagrams have less straightforward interpretations, but any individual diagram can be evaluated using these Feynman rules.

There are also more complicated effects with no obvious diagrammatic interpretation. All of the effects in this section are renormalizations to the first cumulant in the exponent. But presumably higher cumulants of the single-particle density of states can also be renormalized by interactions. We do not know how to systematically investigate these effects. For example, in writing equation (53) we are assuming a density of states where the number of Laplacian eigenvalues between k^2 and $(k + \delta k)^2$ is $\frac{V}{(2\pi)^d} S_{d-1} k^{d-1} \delta k$. More realistically, this density would be a fluctuating variable. Would the overlaps between different eigenstates depend on the relative energies and on the density of states? We don't know. The higher-cumulant analogues of the calculation in this section are an open question.

7 Discussion and Conclusion

In this paper, we expanded the theory of the hydrodynamic spectral form factor to the more realistic case of second-order hydrodynamics. This more sophisticated theory and its accompanying sound pole structure allowed a new phenomenon: interference in the emergent hydrodynamic SFF formalism. We discovered a variety of different interference patterns, all connecting intimately with the SFF of a single particle problem in various cavities. The expected spectral form factor depends sensitively on both the dimensionality of the system as well as whether the cavity supports chaotic or integrable billiard dynamics.

This opens the gates for calculations in a wide array of settings, including CFTs (which necessarily have both momentum and energy conservation) and systems with spontaneously broken symmetry. In particular, CFTs on spheres have been shown [34] to have eternal non-decaying hydrodynamic modes. These would lead to strong enhancements in the SFF out to arbitrary times, even into the plateau region.

As our ability to numerically calculate the SFFs of quantum fields theories improves [35], one might look for at least the leading peaks in a numerical spectral form factor. One highly optimistic possibility is that signatures of these results could be found in the original home of Wigner-Dyson statistics: atomic nuclei. These nuclei are hydrodynamic systems with vibrational modes, these modes might have a signature in the spectral form factor.

An important direction for future work is seeing whether this emergent spectral effect can give rise to enhanced 2-point functions in the CTP hydrodynamic theory. Figure (8) shows a diagram which depends on an internal integral over the frequencies of the two legs. If the two-point function of these frequencies is not analytic (as is the case for both integrable and Wigner-Dyson spectral statistics), that leads to a long-time tail (albeit suppressed by a factor of volume).

This work was supported by the Joint Quantum Institute (M.W.) and by the AFOSR under FA9550-19-1-0360 (B.G.S.).

A SYK2 At Finite Temperature

In [13, 14] the authors investigated the many-body SFF in a specific system of free-fermions with random two-body interactions. They find an exponential ramp in the infinite-temperature SFF, in particular with a ramp of the form $SFF \propto N^{\#T}$, where the number depended on the specific model under consideration. This exponential ramp behavior can be argued to come from the same cumulant expansion as equation 49.

In the case of the SYK2 model with no charge/number conservation, we have

$$H = \frac{1}{2} \psi_i M^{ij} \psi_j, \quad (57)$$

where M is an anti-symmetric real matrix. One can show that the eigenvalues of M follow a semicircle law, and obey GUE level repulsion (the reason for this is that even though the matrix is real, the eigenvalues come in pairs $\pm\lambda$, and there is repulsion for both the positive and negative eigenvalues). We can write the full-system SFF at inverse temperature β as

$$\log SFF = \sum_{\lambda > 0} 2\text{Re} \log(1 + \exp(-\beta\lambda + iT\lambda)) = \sum_{j \neq 0} \frac{(-1)^j}{j} \sum_{\lambda > 0} \exp(-\beta j\lambda + ijT\lambda) = \sum_{j \neq 0} \frac{(-1)^j}{j} Z(jT, j\beta) \quad (58)$$

Note the similarity between this form and equation (37). And while at infinite temperature all terms of the cumulant expansion are needed, we will show that at finite temperature only the first two are important.

For most random matrix ensembles, we can write the probability density as

$$dP(M) = \exp(-N \text{tr} V(M)) dM. \quad (59)$$

In terms of the eigenvalues density $\rho(\lambda) = \frac{1}{N} \sum_i \delta(\lambda - \lambda_i)$ and the eigenvalues distribution density as

$$dP(\rho) \propto \exp\left(-\int N^2 V(\lambda) \rho(\lambda) d\lambda + \int N^2 \rho(\lambda_1) \rho(\lambda_2) \log |\lambda_1 - \lambda_2| d\lambda_1 d\lambda_2 + \int N \rho(\lambda) \log \rho(\lambda) d\lambda\right) \mathcal{D}\rho \quad (60)$$

At large N , this is the quadratic functional

$$dP(\rho) = \exp\left(-\int N^2 V(\lambda) \rho(\lambda) d\lambda + \int N^2 \rho(\lambda_1) \rho(\lambda_2) \log |\lambda_1 - \lambda_2| d\lambda_1 d\lambda_2\right) \mathcal{D}\rho. \quad (61)$$

This means that we can analyze quantities related to ρ by linear transformations (including $Z(T, f)$, or the resolvent R) using only the first two cumulants. This breaks down only when ρ gets extremely close to zero. Let us start with $\rho = \bar{\rho}$, the saddle point, and see what temperatures cause trouble.

For instance, the SFF of the SYK2 model can be written

$$SFF = \int dP(\rho) \exp\left(N \int \rho \log(1 + \exp(iT\lambda - \beta\lambda)) d\lambda + cc\right) \quad (62)$$

We can make use of

$$\log(1 + e^{ix}) = \sum_n \log \frac{x - (2n+1)\pi}{(2n+1)\pi} \quad (63)$$

This means we can write the SFF as

$$SFF = \int dP(\rho) \exp\left(N \int \rho \sum_n \log \frac{x - (2n+1)\pi/(T+i\beta)}{(2n+1)\pi/(T+i\beta)} + \log \frac{x - (2n+1)\pi/(T-i\beta)}{(2n+1)\pi/(T-i\beta)} d\lambda\right) \quad (64)$$

Combining with the quadratic large N measure in equation (61) we can solve for the new saddle-point value of ρ . We have

$$\rho = \rho_0 + \delta\rho \quad (65)$$

$$\delta\rho = \frac{1}{N} \sum_n (2n+1) \frac{\beta}{T^2 + \beta^2} \frac{1}{\left(x - \frac{(2n+1)\pi T}{T^2 + \beta^2}\right)^2 + (2n+1)^2 \pi^2 \frac{\beta^2}{(T^2 + \beta^2)^2}}$$

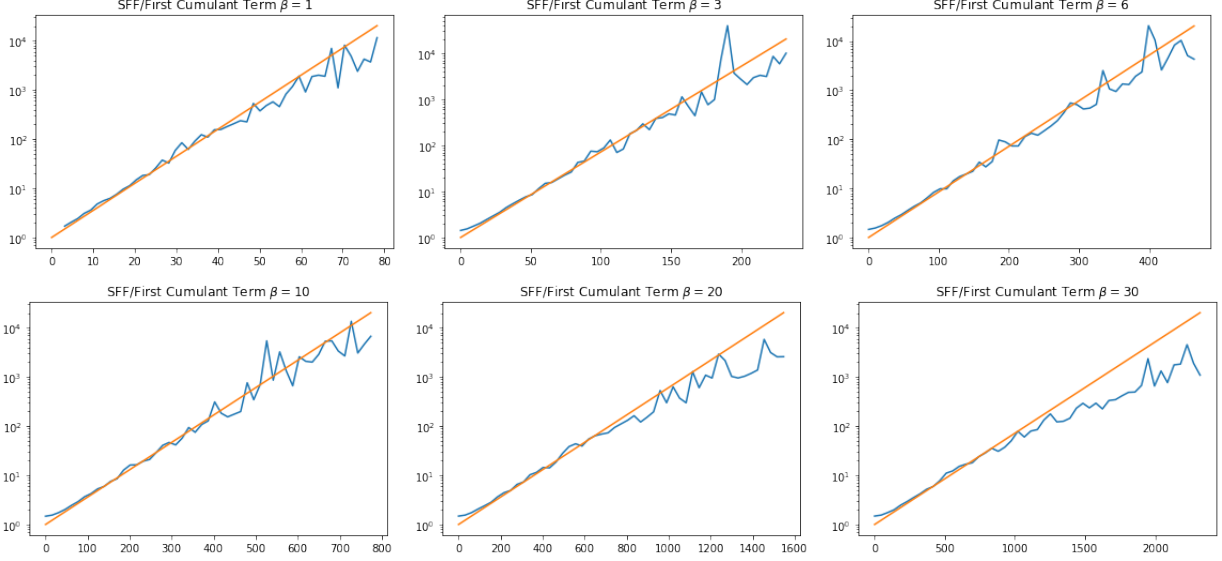


Figure 9: The first two terms in the cumulant expansion seem adequate for the SYK2 model

In the limit of small β , this is just a train of delta functions of mass $\frac{1}{N}$. The deepest well will be of depth $\frac{T^2 + \beta^2}{N\pi^2\beta}$. If this becomes $O(1)$, comparable to ρ_0 , the cumulant expansion breaks down. For any fixed nonzero β this isn't a concern, except at very long times. But if $\beta \sim N^{-1}$, we get the more complicated $N^{\#T}$ behavior.

In the regime where the cumulant expansion works, and where $T \gg \beta$, we can evaluate the first two terms c_1, c_2 in the cumulant expansion. The first is non-universal and dependent on the density of states:

$$c_1 = \mathbb{E} \sum_{j \neq 0} \frac{(-1)^j}{j} Z(ijT - j\beta) = \sum_j (-1)^j j \int d\lambda \rho(\lambda) \exp(ijT\lambda - j\beta\lambda) \quad (66)$$

In the case of the semicircle law, this becomes a sum of Bessel functions.

The next term is

$$c_2 = \text{var} \sum_{j \neq 0} (-1)^j j Z(ijT - j\beta) = \frac{1}{6\pi} \sum_{j \neq 0} \frac{1}{j^2} \int d\lambda \exp(-2j\beta\lambda) jT \quad (67)$$

The sum can be evaluated for any values of the parameters. In the case where $\beta E_{\max} \gg 1$, that sum becomes simple:

$$\text{var} \sum_{j \neq 0} (-1)^j j Z(ijT - j\beta) = \frac{1}{6\pi} \sum_{j \neq 0} \frac{T}{2\beta j^2} = \frac{\pi T}{12\beta} \quad (68)$$

We can graph $\log(\text{SFF}(T, \beta)) - c_1$ and c_2 as functions of time. We see good alignment in figure 9.

References

- [1] F. Haake, *Quantum Signatures of Chaos*. Springer Series in Synergetics. Springer Berlin Heidelberg, 2010.
- [2] O. Bohigas, M. J. Giannoni and C. Schmit, *Characterization of chaotic quantum spectra and universality of level fluctuation laws*, *Phys. Rev. Lett.* **52** (Jan, 1984) 1–4.
- [3] M. Mehta, *Random Matrices*. ISSN. Elsevier Science, 2004.

- [4] F. J. Dyson, *Statistical theory of the energy levels of complex systems. iii*, *Journal of Mathematical Physics* **3** (1962) 166–175, [<https://doi.org/10.1063/1.1703775>].
- [5] E. Wigner and J. Griffin, *Group Theory and Its Application to the Quantum Mechanics of Atomic Spectra*. Pure and applied Physics. Academic Press, 1959.
- [6] O. Bohigas and M.-J. Giannoni, *Chaotic motion and random matrix theories*, in *Mathematical and computational methods in nuclear physics*, pp. 1–99. Springer, 1984.
- [7] R. Dubertrand and S. Müller, *Spectral statistics of chaotic many-body systems*, *New Journal of Physics* **18** (2016) 033009.
- [8] B. Bertini, P. Kos and T. c. v. Prosen, *Exact spectral form factor in a minimal model of many-body quantum chaos*, *Phys. Rev. Lett.* **121** (Dec, 2018) 264101.
- [9] J. S. Cotler, G. Gur-Ari, M. Hanada, J. Polchinski, P. Saad, S. H. Shenker et al., *Black holes and random matrices*, *Journal of High Energy Physics* **2017** (May, 2017) .
- [10] P. Saad, S. H. Shenker and D. Stanford, *A semiclassical ramp in SYK and in gravity*, 1806.06840.
- [11] M. V. Berry and M. Tabor, *Level clustering in the regular spectrum*, *Proceedings of the Royal Society of London. A. Mathematical and Physical Sciences* **356** (1977) 375–394.
- [12] D. Roy and T. Prosen, *Random matrix spectral form factor in kicked interacting fermionic chains*, *Physical Review E* **102** (Dec, 2020) .
- [13] Y. Liao, A. Vikram and V. Galitski, *Many-body level statistics of single-particle quantum chaos*, *Phys. Rev. Lett.* **125** (Dec, 2020) 250601.
- [14] M. Winer, S.-K. Jian and B. Swingle, *Exponential ramp in the quadratic sachdev-ye-kitaev model*, *Physical Review Letters* **125** (dec, 2020) .
- [15] M. Winer and B. Swingle, *The loschmidt spectral form factor*, 2022. 10.48550/ARXIV.2206.00677.
- [16] H. A. Weidenmüller, *Parametric level correlations in random-matrix models*, *Journal of Physics: Condensed Matter* **17** (may, 2005) S1881–S1887.
- [17] T. Guhr, A. Müller-Groeling and H. A. Weidenmüller, *Random-matrix theories in quantum physics: common concepts*, *Physics Reports* **299** (1998) 189–425.
- [18] J. Cotler and K. Jensen, *A precision test of averaging in ads/cft*, 2022. 10.48550/ARXIV.2205.12968.
- [19] B. D. Simons and B. L. Altshuler, *Universal velocity correlations in disordered and chaotic systems*, *Phys. Rev. Lett.* **70** (Jun, 1993) 4063–4066.
- [20] M. Winer and B. Swingle, *Hydrodynamic theory of the connected spectral form factor*, 2020. 10.48550/ARXIV.2012.01436.
- [21] M. Winer and B. Swingle, *Spontaneous symmetry breaking, spectral statistics, and the ramp*, *Physical Review B* **105** (mar, 2022) .
- [22] A. J. Friedman, A. Chan, A. De Luca and J. Chalker, *Spectral statistics and many-body quantum chaos with conserved charge*, *Physical Review Letters* **123** (Nov, 2019) .
- [23] S. Moudgalya, A. Prem, D. A. Huse and A. Chan, *Spectral statistics in constrained many-body quantum chaotic systems*, 2020.
- [24] A. Altland and M. R. Zirnbauer, *Nonstandard symmetry classes in mesoscopic normal-superconducting hybrid structures*, *Phys. Rev. B* **55** (Jan, 1997) 1142–1161.
- [25] T. Tao, *Topics in Random Matrix Theory*. Graduate studies in mathematics. American Mathematical Society, 2012.

- [26] H. Liu and P. Glorioso, *Lectures on non-equilibrium effective field theories and fluctuating hydrodynamics*, *PoS TASI2017* (2018) 008, [1805.09331].
- [27] M. Crossley, P. Glorioso and H. Liu, *Effective field theory of dissipative fluids*, *JHEP* **09** (2017) 095, [1511.03646].
- [28] P. Glorioso, M. Crossley and H. Liu, *Effective field theory of dissipative fluids (ii): classical limit, dynamical kms symmetry and entropy current*, *Journal of High Energy Physics* **2017** (Sep, 2017) 1–44.
- [29] P. Gao, P. Glorioso and H. Liu, *Ghostbusters: Unitarity and Causality of Non-equilibrium Effective Field Theories*, *JHEP* **03** (2020) 040, [1803.10778].
- [30] S. Grozdanov and J. Polonyi, *Viscosity and dissipative hydrodynamics from effective field theory*, *Physical Review D* **91** (May, 2015) .
- [31] P. Kovtun, *Lectures on hydrodynamic fluctuations in relativistic theories*, *Journal of Physics A: Mathematical and Theoretical* **45** (Nov, 2012) 473001.
- [32] S. Dubovsky, L. Hui, A. Nicolis and D. T. Son, *Effective field theory for hydrodynamics: Thermodynamics, and the derivative expansion*, *Physical Review D* **85** (Apr, 2012) .
- [33] S. Endlich, A. Nicolis, R. A. Porto and J. Wang, *Dissipation in the effective field theory for hydrodynamics: First-order effects*, *Physical Review D* **88** (Nov, 2013) .
- [34] B. Freivogel, J. McGreevy and S. J. Suh, *Exactly stable collective oscillations in conformal field theory*, *Physical Review D* **85** (may, 2012) .
- [35] L. V. Delacretaz, A. L. Fitzpatrick, E. Katz and M. T. Walters, *Thermalization and chaos in a 1+1d qft*, 2022. 10.48550/ARXIV.2207.11261.